ISSN: 2229-7359 Vol. 11 No. 24s, 2025

https://theaspd.com/index.php

# Impact Of Tio2 On Physical And Optical Properties Of Borosilicate Glasses

Hariom Kumar Kaushik<sup>1,2</sup>, Vijay Garg<sup>2,3</sup>, Km Abida<sup>4\*\*</sup>, Savidh Khan<sup>5\*</sup>, Sushil Kumar<sup>6</sup>, Aditya Sharma<sup>7</sup> Department of Physics, Mahamana Malviya (M.M.) Degree College, Khekra, Bagpat, C.C.S. University Meerut-250004, India.

<sup>2</sup>Department of Physics, M. M. College Modinagar, Ghaziabad, C.C.S. University, Meerut-250004, India.

<sup>3</sup>K. D. College Simbhaoli, Hapur, C.C.S. University, Meerut 250001, India.

<sup>4</sup>Department of Chemistry, KVSCOS, Swami Vivekanand Subharti University, Meerut-250005, Uttar Pradesh, India

<sup>5</sup>Department of Physics and Material Science, Thapar Institute of Engineering and Technology, Patiala-147004, Punjab, India.

<sup>6</sup>Department of Physics, Dhanauri PG College Dhanauri, Haridwar-247667, Uttrakhand.

<sup>7</sup>School of science, IIMT University Meerut.

#### **ABSTRACT**

The effect of  $TiO_2$  into a borosilicate glass matrix is investigated for structural and optical properties. Glass samples with varying TMO concentrations were prepared using the melt-quench technique. X-ray diffraction confirmed the amorphous nature of the synthesized samples. The FTIR studies showed structural changes with  $TiO_2$  addition. The UV-Vi's spectroscopy demonstrated a red shift in optical absorption profiles. The optical band gap and Urbach energy are also discussed. The improved optical properties of the prepared samples were observed on  $TiO_2$  doping.

Keywords: Borosilicate glass, Optical band gap, Dielectric constant, FTIR spectroscopy, and XRD

#### **INTRODUCTION**

In today's context, glasses have become decisive materials due to their innumerable applications. Glasses due to amorphous nature have exceptional properties. They have exceptional optical properties, dielectric properties, transparency, high corrosion and chemical resistance etc. Now, these properties have extensively useful applications in optoelectronics, photonics, radiation shields, laser industry, aerospace industry, defensive coating for metals, luminescent materials, optical fiber communications, useful bioactive materials etc [1-5].

The borosilicate oxide (BS) glass network is made up of two subsystems. The first subsystem consists of boron network in which trigonal coordination BO<sub>3</sub> and fourfold tetrahedral coordination BO<sub>4</sub> unit exists. The trigonal coordination BO<sub>3</sub> can be connected via oxygen atom to form borate bridging oxygen (B-O-B). Along with this, the second subsystem consists of silicate network SiO<sub>2</sub> which has four electrons in its valence band. These electrons could be connected together to form four covalent bonds with non-bridging oxygen (NBO) atoms to form SiO<sub>4</sub> tetrahedra. These two sub-networks of boron and silicate are interconnected to develop Si-O-B covalent bonds [6, 7]. They are most widely utilized types of glasses. The main properties of BS glasses are outstanding chemical durability, good transparency and low coefficients of thermal expansion etc. These glasses have a wide range of applications such as laboratory glassware, utensils, glass used in medical devices, thermal shock-resistant containers, chemically resistant containers, substrate for liquid crystal displays, glasses and optical components for various applications [8-10].

Taha et al. [11] prepared the glasses 55  $B_2O_3$ -35  $Li_2O$ -10 ZnO- $xTiO_2$  (where x = 0, 1, 2, 3 and 4,  $TiO_2$  wt %) by melt quench method. The XRD results showed no any crystalline peak for all the five glass samples. This confirms the amorphous nature of  $TiO_2$  doped borate glasses. The decrease in optical band gaps (3.04-3.02 eV) and increase in urbach energy (1.01-0.67 eV) was seen. The refractive index and dielectric constant vary with increasing wavelength. These variations show interactions between photons and electrons. Finally, authors suggested borate glasses (doped with  $TiO_2$ ) as having good scope in optoelectronic devices.

Herein, two glass samples with increased concentration of  $TiO_2$  in composition  $30SiO_2$ - $50B_2O_3$ -(1-x) Li<sub>2</sub>O- $xTiO_2$  (x = 1.0 and 2.0 mol %) were synthesized via the melt quench technique. Various properties such

ISSN: 2229-7359 Vol. 11 No. 24s, 2025

https://theaspd.com/index.php

as physical, structural, optical properties of samples were studied using XRD, FTIR spectroscopy, UVvisible spectroscopy etc. Based on these results the impact of transition metal oxide (TiO<sub>2</sub>) on optical, structural and physical properties of borosilicate glass was provided in this paper. Further, the optical behavior of all fabricated glass samples was examined in view of their useful applications in fabrication of optoelectronic devices.

#### 2.0 EXPERIMENTAL WORK

## 2.1 Synthesis of glasses

In present work a series of glasses with composition  $50B_2O_3$ - $30SiO_2$ -(20-x) Li<sub>2</sub>O-xTiO<sub>2</sub> (where, x = 1.0 and 2.0 mol %) were synthesized using melt-quench method. This series of two samples were named as LT 1.0 (x=1.0) and LT 2.0 (x=2.0). The starting chemicals (H<sub>3</sub>BO<sub>3</sub>, Li<sub>2</sub>O, SiO<sub>2</sub>, and TiO<sub>2</sub>) were used of 99.99% purity from Sigma-Aldrich Company. The Appropriate amounts of SiO<sub>2</sub>, H<sub>3</sub>BO<sub>3</sub>, Li<sub>2</sub>O, and TiO<sub>2</sub> were mixed and ground using acetone medium in an agate mortar and pestle for 2.5 hours. The powder so obtained was taken in high grade alumina crucible and melted in a high resistance programmable furnace at 1550 °C. The melt so obtained was quenched by pouring it between two copper thick plates at room temperature. The quenched samples are kept for annealing (at 450 °C) in muffle furnace for 4 h to remove stresses produced due to rapid cooling.

#### 2.2 Characterization techniques

o check the amorphous nature of so prepared samples, the XRD analysis was employed. X-ray diffraction analysis of the powdered glass samples was performed by a PANalytical X' Pert Pro MPD diffractometer. The Cu-K $\alpha$  radiations ( $\lambda = 1.54$  Å) is used with a scan rate of  $2^{\circ}$ / minute. The Fourier transform infrared transmission spectra of all Ti-doped glasses were recorded at room temperature in the wave number range 400-2000 cm<sup>-1</sup> by a Shimadzu FTIR-8001 Fourier-transform computerized infrared spectrometer. The IR transmission measurements were using the KBr pellet technique. A double beam UV-Vis spectrophotometer (Model: Hitachi 3900 H) is used to record the absorption and diffused reflectance spectra (DRS) of powder samples in the wavelength range of 200-800 nm.

# 3. RESULTS AND DISCUSSION

#### 3.1 Physical Parameters

The density  $(\rho)$  of Ti-doped samples at room temperature was computed by employing Archimedes principle with xylene as buoyant liquid using following equation [12];

$$\rho = \rho_{xylene} \times \frac{w_{air}}{(w_{air} - w_{xylene})}$$
 (1)

 $\rho = \rho_{xylene} \times \frac{w_{air}}{(w_{air} - w_{xylene})} \tag{1}$  where,  $w_{xylene}$  and  $w_{air}$  are the weight of the sample in xylene and air respectively and  $\rho_{xylene}$  is the density of xylene (0.863 gcm<sup>-3</sup>) at room temperature.

$$V_{\rm m} = \frac{\sum_{\rm i} M_{\rm i}}{\rho} \ {\rm cm}^3 \ {\rm mole}^{-1} \tag{2}$$

The molar volume ( $V_m$ ) of TiO<sub>2</sub>-doped glass samples was estimated using the following equation [12]:  $V_m = \frac{\sum_i M_i}{\rho} \text{ cm}^3 \text{ mole}^{-1} \tag{2}$  Where,  $\sum_i M_i$  the sum of molar masses of constituent oxides and  $\rho$  is the density of the samples, respectively. The obtained physical parameters of all as quench glass samples are displayed in Table 1. The density (p) of composition  $50B_2O_3$ - $30SiO_2$ -(20-x) Li<sub>2</sub>O-xTiO<sub>2</sub> (where x = 1.0 and 2.0 mol %) increases  $(2.32 \text{ to } 2.39 \text{ g/cm}^3)$  as concentration of TiO<sub>2</sub> increases from 1.0 to 2.0 mol% at the expense of TiO<sub>2</sub> content. The density is an additive nature [13] and increasing with an increase in doping of TiO<sub>2</sub> which is due to the 2.11 times density of TiO<sub>2</sub> (4.26 g/cm<sup>3</sup>) than Li<sub>2</sub>O (2.01 g/cm<sup>3</sup>). The molar volume decreases (25.56-25.02 cm<sup>3</sup>/mol) with the doping of TiO<sub>2</sub> at the expense of Li<sub>2</sub>O content. The Molar volume depends on molecular weight and density. The density and molar volume have reciprocal relation to each other as shown in equation (2). In present samples, molar volume and density show general behavior i.e. density increases whereas molar volume decreases.

For present samples, the variation of ionic concentration  $(N_{Ti})$  and inter-ionic distance (Ti) as a function of  $TiO_2$  concentration for  $50B_2O_3$ - $30SiO_2$ (20-x)  $Li_2O$ -x $TiO_2$  (where x = 1.0 and 2.0 mol %) glass compositions is given in table 1. It is observed that titanium ion  $(Ti^{4*})$  concentration  $(N_{Ti})$  increases, whereas inter-ionic distance (R<sub>Ti</sub>) decreases on addition of TiO<sub>2</sub> in the place of Li<sub>2</sub>O.

ISSN: 2229-7359 Vol. 11 No. 24s, 2025

https://theaspd.com/index.php

Table 1: Summery of physical parameters of Titanium-doped lithium borosilicate glasses with their labels.

Physical parameters	LT 1.0	LT 2.0	
Molar mass, M (g mole <sup>-1</sup> )	59.309	59.809	
Molar volume, V <sub>m</sub> (cm <sup>3</sup> mol <sup>-1</sup> )	25.564	25.024	
Density, $\rho$ (g cm <sup>-3</sup> )	2.32	2.39	
Molar volume of oxygen, V <sub>o</sub> (cm <sup>3</sup> mol <sup>1</sup> )	11.066	10.786	
Oxygen Packing density, OPD (mol litre <sup>-1</sup> )	90.36	92.71	
Lithium Ionic concentration, N <sub>Li</sub> (×10 <sup>21</sup> cm <sup>-3</sup> )	4.47	4.33	
Lithium Inter-ionic distance, R <sub>Li</sub> (Á)	6.06	6.13	
Titanium Ionic concentration, N <sub>Fe</sub> (×10 <sup>20</sup> cm <sup>-3</sup> )	9.42	19.25	
Titanium Inter-ionic distance, R <sub>Fe</sub> (Å)	10.20	8.03	

#### 3.2 Structural Properties

#### 3.2.1 X-ray diffraction (XRD) analysis

The XRD patterns of as-quench samples with  $TiO_2$  content (where x = 1.0 and 2.0 mol %) are shown in Fig. 1.

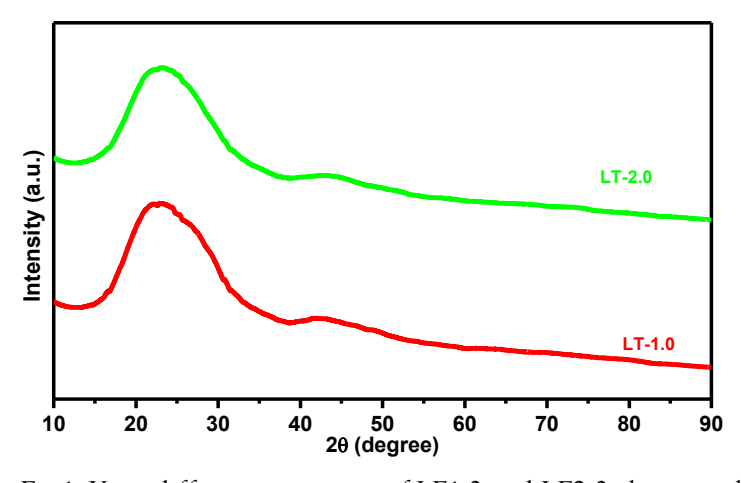


Fig.1. X-ray diffraction patterns of LF1.0 and LF2.0 glass samples

The XRD patterns of these samples do not show any sharp peaks, which confirm the amorphous nature of all the prepared samples. Moreover, the XRD patterns of glass samples show a broad halo centered at 22.12°, which also indicates the short-range order characteristics of a glassy amorphous material.

## 3.2 Optical Properties

## 3.2.1 Absorbance and optical band gap

ISSN: 2229-7359 Vol. 11 No. 24s, 2025

https://theaspd.com/index.php

In absorption spectra of the prepared glass samples show strong absorption around 250-280 nm wavelength as shown in Fig. 2. The absorption band around 250-280 nm confirms the presence of titanium ion most predominantly in  $\text{Ti}^{4+}$  state.

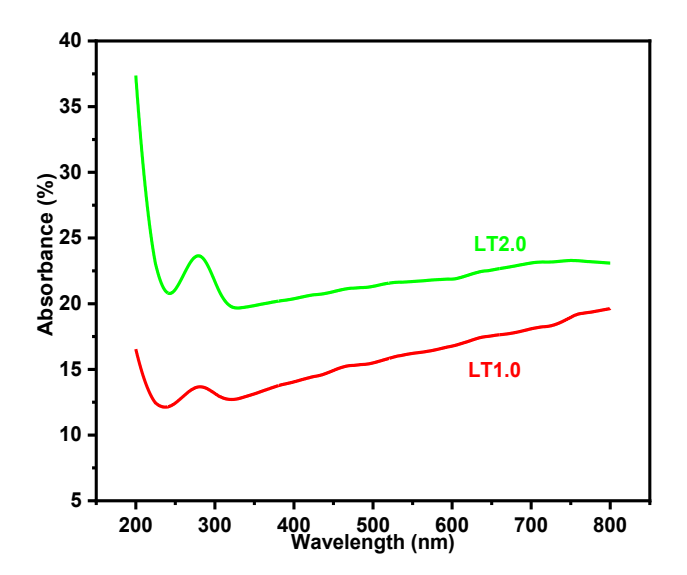


Fig. 2. Variation in absorbance with wavelength of titanium oxide doped borosilicate glass samples. The light absorption coefficient ( $\alpha$ ) can be calculated for all the prepared glass samples as follows:  $\alpha(\nu) = A/t$  (3)

Here, A and t refer to the sample's absorbance and thickness, respectively.

The UV-Visible-NIR spectrophotometer is used to determine the amount of radiation absorbed by a material over the wavelength range 200-800 nm. The optical absorption and band edge characteristics provide valuable information about the energy gap and band structure of glass materials [14]. The optical band gap is calculated with the help of absorption coefficient ( $\alpha$ ) at the absorption edge by the following relation as suggested by Tauc and explained by Davis and Mott [15, 16].

$$\alpha h v = A \big( h v - E_{opt} \big)^n \tag{4}$$

Where n is the index number, A is called the band tailing parameter (a constant), hv is the input photon energy, and  $\alpha$  is the absorption coefficient. The exponent term (n) can have values 2, 3, 1/2 and 3/2 which corresponds to indirect allowed, indirect forbidden, direct allowed and direct forbidden transitions, respectively. The optical band gap was determined for indirect allowed transitions (n = 2), by extrapolating the best linear fit of Tauc plot between ( $\alpha hv$ )<sup>2</sup> vs phonon energy (hv) (Fig. 3 a & b).

ISSN: 2229-7359 Vol. 11 No. 24s, 2025

https://theaspd.com/index.php

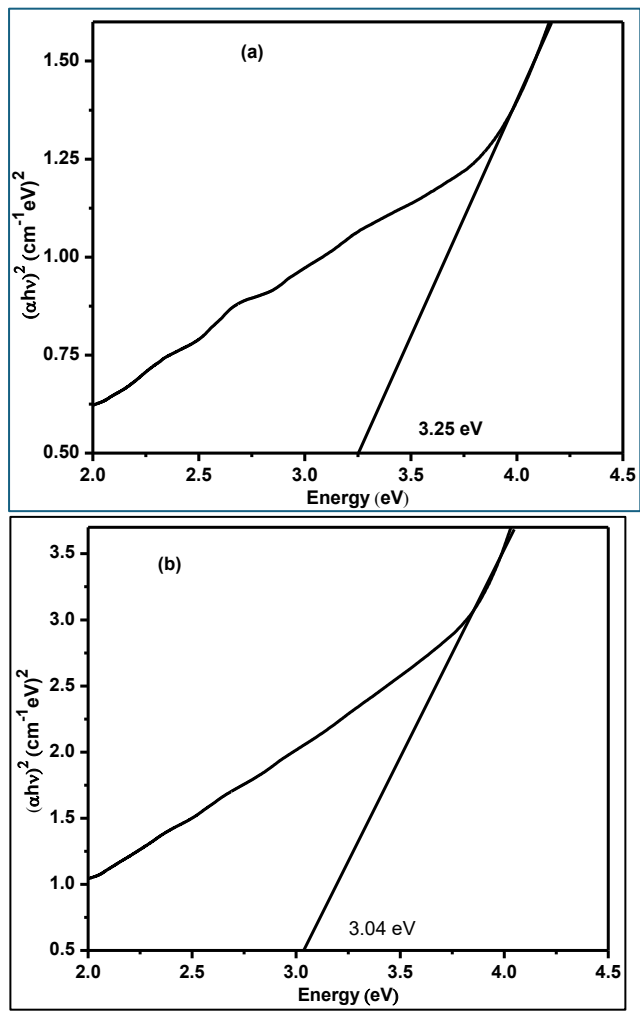


Fig. 3. Optical band gap measurement of titanium oxide doped borosilicate (a) LT1.0 and (b) LT2.0 glass samples using Tauc plot.

The optical band gap experiences a decrease from 3.25 eV to 3.04 eV with the addition of  $TiO_2$  (1.0 to 2.0 mol%) at the expense of  $Li_2O$  content (Table 2). The sample with the lowest concentration of  $TiO_2$  (x=1.0) shows the highest optical band gap (3.25 eV) while the sample with the highest concentration of  $TiO_2$  (x=2.0) shows the lowest optical band gap (3.04 eV). This decrease in  $E_{opt}$  is due to an increase in non-bridging oxygens (NBOs). The similar kind of decrease in  $E_{opt}$  with the introduction of CuO in borosilicate glasses is also reported by Kaushik et al. [10].

#### 3.2.2 Urbach energy

The irregularity in the band gap of glass samples are measured in terms of Urbach energy. The Urbach energy is shown by  $\Delta E$  and determined using the following equations.

$$\alpha(\nu) = \beta \cdot \exp(h\nu/\Delta E)$$
and
$$\ln \alpha(\nu) = (h\nu/\Delta E) + C$$
(6)

Where h is the Planck constant,  $\beta$  is also a constant,  $\nu$  is photon frequency and C stands for a constant. The Urbach energy is determined by examining the inclination of the linear portions in the ln ( $\alpha$ ) versus the energy ( $h\nu$ ) curves. The values of Urbach energy are shown in Table 2. The Urbach energy increases from 4.95 to 9.27 eV with the TiO<sub>2</sub> addition. Therefore, the disorderness increases due to an increase in NBOs, anomalous bonds creation and dangling bonds in glass samples [10, 13, 17, 18].

Table 2: Optical parameters of Titanium -doped lithium borosilicate glasses with their labels:

Optical parameters	LF 1.0	LF 2.0
Band gap (E <sub>g</sub> ) (eV)	3.25	3.04

ISSN: 2229-7359 Vol. 11 No. 24s, 2025

https://theaspd.com/index.php

Urbach Energy (eV)	4.95	9.27

#### 3.2.3 Refractive index and extinction coefficient determination

The refractive index of a material plays vital role in optical devices design. It finds wide applications in optical switches, optical filters and modulators, etc. Its real part is reciprocal to wave propagation velocity. The imaginary part of refractive index gives information about attenuation of electromagnetic wave [19]. The refractive index is termed as a complex function (N) of wavelength in the following form:

$$N = n - ik \tag{7}$$

Where, the complex refractive index (N) having two parts namely n is the real part of N and k is the imaginary part of N. The real refractive index (n) of melt quench glasses with the doping of  $TiO_2$  on the cost of  $Li_2O$  is estimated using reflectance (R) as follows [20];

$$R = \frac{(n-1)^2 + k^2}{(n+1)^2 + k^2} \tag{8}$$

If  $k \le n$ , equation (8) is reduced to

$$n = \frac{1 + \sqrt{R}}{1 - \sqrt{R}} \tag{9}$$

The variation of refractive index (n) of all the prepared glasses as a function of wavelength in the range of 200-800 nm is shown in Fig. 4(a). The refractive index decreases with increasing wavelength ( $\lambda$ ) which shows its normal dispersion behavior. The refractive index of the prepared glass samples increases (from 5.59 to 5.69) with increasing TiO<sub>2</sub> content. The change in refractive index depends on the several factors such as density, concentration of heavy metal, polarizability and NBOs etc [21, 22]. The increase in refractive index with increasing TiO<sub>2</sub> content is due to the higher density and molar mass of TiO<sub>2</sub> (79.86 g/mol) than Li<sub>2</sub>O (29.88 g/mol). The increase in the refractive index can also be due to an increase in the number of non-bridging oxygen.

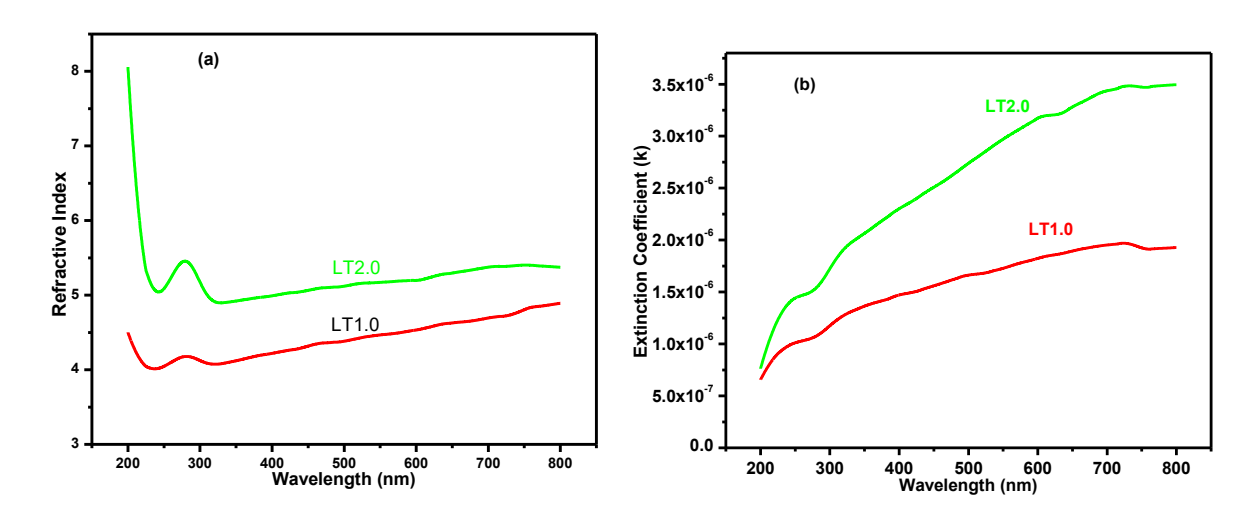


Fig. 4. Change in (a) refractive index and (b) extinction coefficient with wavelength of LT1.0 and LT2.0 glass samples

The extinction coefficient (k) was calculated from the reported relation as follows:

$$k = \frac{\alpha\lambda}{4\pi} \tag{10}$$

Where,  $\lambda$  is the wavelength of incident radiation. The variation of k of all the prepared glasses as a function of wavelength in the range of 200-800 nm is shown in Fig. 4(b). The extinction coefficient (k) gives the total optical loss caused by scattering, absorption, transmittance etc. The extinction coefficient of as quench glasses increases with increasing wavelength from 200 to 800 nm. The extinction coefficient is also found to be increased with increasing  $TiO_2$  concentration [23]. Similar kind results also reported by Kaushik et al. [24].

ISSN: 2229-7359 Vol. 11 No. 24s, 2025

https://theaspd.com/index.php

## **CONCLUSION**

The structural and optical properties of  $TiO_2$  doped borosilicate glasses examined. Physical properties such as density, molar volume, ionic concentration (Ti) and their inter-ionic distance are discussed. The x-ray diffraction pattern suggests glass nature of the prepared samples. The FTIR spectra confirm the conversion of  $BO_3$  structural units into  $BO_4$  units on addition of  $Ti_2O_1$ . The band gap energy varies from 3.25 eV to 3.04 eV. The refractive index increases with an increase in  $TiO_2$  doping. The Urbach energy shows an increasing trend along with the  $TiO_2$  concentration.

## Conflicts of interest

There are no competing interests to disclose.

#### Acknowledgment

Authors are thankful to the Panjab University, Chandigarh, for providing the characterizations facilities.

#### Funding sources

Public, private, or nonprofit funding organisations did not provide any specific grants for this study.

#### REFERENCES

- 1. M.I. Sayyed, M. Rashad, C.V. More, A. Kumar, Preparation and radiation shielding features of high density, transparent borosilicate glasses with different Bi2O3 contents, Nucl. Eng. Technol. 56 (2024) 5043-5047, https://doi.org/10.1016/j.net.2024.07.013
- 2. C.A. Nieves, M.T. Lanagan, Exploring the dielectric polarization and ionic conduction mechanisms in sodium-containing silicate and borosilicate glasses, J.Non-Cryst. Solids 617 (2023) 122505. https://doi.org/10.1016/j.jnoncrysol.2023.122505
- 3. Y.S. Hordieiev, A.V. Zaichuk, Structure, thermal and crystallization behavior of lead-bismuth silicate glasses, Results Mater. 19 (2023) 100442. https://doi.org/10.1016/j.rinma.2023.100442
- 4. V. D, D. C, U. Deka, A comprehensive review of structural, and optical properties of boronated glasses doped with 3-d transition metal oxides (TMOs), J. Alloys and Compd 1024 (2025) 180145. https://doi.org/10.1016/j.jallcom.2025.180145
- 5. R. Samudrala, A. Azeem P, V. Penugurti, B. Manavathi, Cytocompatibility studies of titania-doped calcium borosilicate bioactive glasses in-vitro, Mater. Sci. Eng. C 77 (2017) 772-779. http://dx.doi.org/10.1016/j.msec.2017.03.245
- 6. S. A. Al Kiey, S. A. M. Abdel-Hameed, M. A. Marzouk, Influence of Transition Metals on the Development of Semiconducting and Low Thermal Expansion TiO2 Borosilicate Glasses and Glass Ceramics, Silicon 16 (2024) 2945-2953. https://doi.org/10.1007/s12633-024-02896-y
- 7. F.A. Wahab, M.A. Baki, S.Ibrahim, M. Abdelnabi, H. Abdelmaksoud, Investigation of oxygen defects in chromium doped borosilicate glass co-doped with alkali metal (Na2O) and transition metal (ZnO) for photonic applications, Appl. Phys. A 131 70 (2025) https://doi.org/10.1007/s00339-024-08114-1
- 8. K. Thieme, A. Herrmann, B. Topper, T. Hoche, Effect of composition and phase separation on structure and luminescence properties of Tb3+ doped borosilicate glasses, Opt. Mater. 159 (2025) 116518. https://doi.org/10.1016/j.optmat.2024.116518
- 9. J.S. Kumar, V. Madhuri, J.L. Kumari, Spectral Studies of Vanadyl-Doped Cadmium Strontium Borosilicate Glass System. Appl. Magn. Reson. 44 (2013) 479-494. https://doi.org/10.1007/s00723-012-0409-7
- 10. S. Cheng, G. Yang, Y. Zhao, M.Y. Peng, J. Skibsted, Y. Yue, Quantification of the boron speciation in alkali borosilicate glasses by electron energy loss spectroscopy, Sci Rep 5 (2015) 17526. https://doi.org/10.1038/srep17526
- 11. T.A. Taha, Y.S. Rammah, Optical characterization of new borate glass doped with titanium oxide, J Mater Sci: Mater Electron, 27 (2016) 1384-1390. https://doi.org/10.1007/s10854-015-3901-7
- 12. S. Singh, G. Kalia, K.Singh, Effect of intermediate oxide (Y2O3) on thermal, structural and optical properties of lithium borosilicate glasses, J. Mol. Struct 1086 (2015) 239-245. http://dx.doi.org/10.1016/j.molstruc.2015.01.031
- 13. N. Bansal, S. Khan, G. Sharma, Rajni, D. Kumar, K. Singh, Alkali field strength effects on optical, dielectric, and conducting properties of calcium borosilicate glasses, Ceram Int 49 (2023) 2998–3006 https://doi.org/10.1016/j.ceramint.2022.09.284
- 14. H.K. Kaushik, A. Kaur, V. Garg, K. Abida, S. Kumar, K. Singh, S.P. Singh, S. Khan, Effect of CuO on physical, structural and optical properties of lithium borosilicate glasses, Mater Today Commun 35 (2023) 106208, https://doi.org/10.1016/j.mtcomm.2023.106208
- 15. S. Khan, K. Singh, Effect of TiO2 doping on structural and electrical properties of melt-quench V2-x TixO5- $\boldsymbol{\delta}$ , 0.15  $\leq$  x  $\leq$  0.30 systems, J Mater Sci: Mater Electron, 32 (2021) 12594-12607. https://doi.org/10.1007/s10854-021-05896-5
- 16. S. Khan, G. Kaur, K. Singh, Effect of ZrO2 on dielectric, optical and structural properties of yttrium calcium borosilicate glasses, Ceram. Int. 43 (2017) 722-727. http://dx.doi.org/10.1016/j.ceramint.2016.09.219
- 17. V. Raghuvanshi, I. Rashmi, A. Ingle , H.D. Shashikala , H.S. Nagaraja, A comprehensive study uncovering physical, structural, and optical properties of Cu2O and TiO2-reinforced borosilicate glasses as optical filters, Opt. Mater. 153 (2024) 115601. https://doi.org/10.1016/j.optmat.2024.115601
- 18. N. Chutithanapanon, C. Bootjomchai, R. Laopaiboon, Investigation of the optical properties of borosilicate glass recycled from high-pressure sodium lamp glass: Compositional dependence by addition of Bi2O3, Journal of Physics and Chemistry of Solids 132 (2019) 244-291, doi: https://doi.org/10.1016/j.jpcs.2019.05.005.
- 19. M. Medhat, S.Y. El-Zaiat, A.M. Fayad, F.A. Moustafa, M.A. Shirif, Effect of titanium dioxide doping on optical properties of borosilicate photochromic glasses, Silicon 10 (2018) 525-536. https://doi.org/10.1007/s12633-016-9484-y

ISSN: 2229-7359 Vol. 11 No. 24s, 2025

https://theaspd.com/index.php

20. S.Y. El-Zaiat, M.B. El-Den, S.U. El-Kameesy, Y.A. El-Gammam, Spectral dispersion of linear optical properties for Sm2O3 doped B2O3-PbO-Al2O3 glasses Opt. Laser Technol 44 (2012) 1270-1276. https://doi.org/10.1016/j.optlastec.2011.12.051

- 21. M.G. Moustafa, M.Y. Hassaan, Optical and dielectric properties of transparent ZrO2-TiO2-Li2B4O7 glass system J. Alloys Compd 710 (2017) 312-322, http://dx.doi.org/10.1016/j.jallcom.2017.03.192
- 22. R. Kaur, R.B. Rakesh, S.G. Mhatre, V. Bhatia, D. Kumar, H. Singh, S.P. Singh, A. Kumar, Physical, optical, structural and thermoluminescence behaviour of borosilicate glasses doped with trivalent neodymium ions, Opt. Mater. 117 (2021) 111109. https://doi.org/10.1016/j.optmat.2021.111109
- 23. Y.B. Saddeek, E. R. Shaaban, E.S. Moustafa, H. M. Moustafa, Spectroscopic properties, electronic polarizability, and optical basicity of Bi2O3-Li2O-B2O3 glasses, Physica B 403 (2008) 2399-2407. https://doi.org/10.1016/j.physb.2007.12.027
- 24. H.K. Kaushik, S. Kumar, M.G. Chaudhary, S. Khan, Optical properties of CdS:Pb thin layer deposited on glass substrate, Indian J. Pure Appl. Phys. 58 (2020) 11-15. http://nopr.niscair.res.in/handle/123456789/53478